Wiring Photosystem I for Direct Solar Hydrogen Production[†]

Carolyn E. Lubner,[‡] Rebecca Grimme,[‡] Donald A. Bryant,[§] and John H. Golbeck*,[‡,§]

[‡]*Department of Chemistry, The Pennsylvania State University, University Park, Pennsylvania 16802 and*
[§]*Department of Biochemistry and Molecular Biology, The Pennsylvania State University, University Park, Pennsylvania 16802*

ABSTRACT: The generation of H_2 by the use of solar energy is a promising way to supply humankind's energy needs while simultaneously mitigating environmental concerns that arise due to climate change. The challenge is to find a way to connect a photochemical module that harnesses the sun's energy to a catalytic module that generates H_2 with high quantum yields and rates. In this review, we describe a technology that employs a "molecular wire" to connect a terminal [4Fe-4S] cluster of Photosystem I directly to a catalyst, which can be either a Pt nanoparticle or the distal [4Fe-4S] cluster of an [FeFe]- or [NiFe]-hydrogenase enzyme. The keys to connecting these two moieties are surface-located cysteine residues, which serve as ligands to Fe−S clusters and which can be changed through site-specific mutagenesis to glycine residues, and the use of a molecular wire terminated in sulfhydryl groups to connect the two modules. The sulfhydryl groups at the end of the molecular wire form a direct chemical linkage to a suitable catalyst or can chemically rescue a [4Fe-4S] cluster, thereby generating a strong coordination bond. Specifically, the molecular wire can connect the F_B iron−sulfur cluster of Photosystem I either to a Pt nanoparticle or, by using the same type of genetic modification, to the differentiated iron atom of the distal [4Fe-4S]·$(Cys)_3(Gly)$ cluster of hydrogenase. When electrons are supplied by a sacrificial donor, this technology forms the cathode of a photochemical half-cell that evolves H_2 when illuminated. If such a device were connected to the anode of a photochemical half-cell that oxidizes water, an in vitro solar energy converter could be realized that generates only O_2 and H_2 in the light. A similar methodology can be used to connect Photosystem I to other redox proteins that have surface-located [4Fe-4S] clusters. The controlled light-driven production of strong reductants by such systems can be used to produce other biofuels or to provide mechanistic insights into enzymes catalyzing multielectron, proton-coupled reactions.

An economy based on H_2 depends on utilizing the 143 kJ/g of energy available in the heat of combustion of the reaction $H_2 + \frac{1}{2}O_2 \rightarrow H_2O$. Given that H_2 is technically not a fuel, i.e., it does not exist in minable quantities on Earth, H_2 can be produced by the opposite reaction, but with a minimum energy input of 143 kJ/g. This energy can be derived from the combustion of carbon-based fuels such as natural gas, oil, or coal, or it can be supplied by noncarbonaceous sources such as nuclear, tidal, wind, or solar energy. There are especially compelling reasons for choosing the solar option: sunlight is widely, albeit unevenly, distributed over the Earth's surface; it is plentiful (the solar constant is 1.37 kW/m^2); and it is for all intents and purposes inexhaustible. Moreover, the use of solar energy does not require the combustion of carbon-based fuels, which are increasingly expensive to exploit, which are nonuniformly located on the surface of the Earth, and which lead to global warming because their use increases the CO_2 content of the atmosphere. An additional virtue of H_2 as an alternative energy source is that the product of combustion is H_2O. In spite of these attributes, it should be recognized that

there are serious challenges in converting to a hydrogen economy. One potential problem is that the widespread use of H_2 would require a large change in infrastructure, starting from generation and continuing through storage to distribution and utilization. Although H_2 has nearly three times the energy content of gasoline on a weight basis (120 MJ/kg vs 44 MJ/kg), the situation is reversed on a volume basis (3 MJ/L at 5000 psi or 8 MJ/L as a liquid vs 32 MJ/L for gasoline). This translates to a larger storage, distribution, and utilization system. Another issue is that the H_2 generated would be at atmospheric pressure, and it would need to be compressed, liquefied, or captured as a hydride. Nevertheless, most scientists and engineers working in the field predict that these problems will eventually be overcome. Thus, the foremost problem at present is still finding an economical method for the generation of H_2 from a renewable energy source such as sunlight.

Approximately 2.7 Ga[1] ago, cyanobacteria perfected two types of light-dependent enzymes that carry out the conversion of solar energy into chemical bond energy. One of them, Photosystem II (PS II), performs the half-cell reaction: $H_2O + 2h\nu \rightarrow \frac{1}{2}O_2 + 2H^+ + 2e^-$. The other one, Photosystem I (PS I), catalyzes the

[1]Abbreviations: PS I, Photosystem I; F_X, F_A, and F_B, three [4Fe-4S] clusters of PS I, the last two of which are contained in PsaC; Ga, billion years; PS II, Photosystem II; Cyt *c*, cytochrome *c*; Fd, ferredoxin; H_2ase, hydrogenase; Chl, chlorophyll; P700-F_X core, PS I preparation in which the stromal polypeptides PsaC, PsaD, and PsaE, together with [4Fe-4S] clusters F_A and F_B, have been removed; DPIP, 2,6-dichlorophenolindophenol; PC, plastocyanin; PDB, Protein Data Bank.

light-driven transfer of an electron from reduced cytochrome *c* (Cyt c_{red}) to oxidized ferredoxin (Fd$_{ox}$): Cyt c_{red} + Fd$_{ox}$ + $h\nu$ → Cyt c_{ox} + Fd$_{red}$. Electrons from reduced ferredoxin are directly used to reduce required nutrients or are used to produce the more stable biological reductant, NADPH. The reactions catalyzed by both photosystems are thermodynamically unfavorable but are driven to completion at the expense of the energy of a visible photon. PS II and PS I operate in series so that the complete reaction is carried out: $2H_2O + 2NADP^+ + 4h\nu \rightarrow O_2 + 2H^+ + 2NADPH$. The final product, NADPH, is the biological equivalent of H_2; both are oxygen-stable, and their standard redox potentials are similar (the E'° of the NADP$^+$/NADPH half-cell couple is -324 mV, whereas the E'° of the H^+/H_2 half-cell couple is -414 mV). Although NADPH is an indispensable reductant in living cells, it is not particularly useful as a source of stored bond energy for human activity. However, were it possible to re-engineer PS I to generate H_2 instead of NADPH, a source of stored energy suitable for use in fuel cells would become available.

It is generally acknowledged that a practical device aimed at generating biofuels using light as the energy source requires three components: a photochemical module that converts light energy to either a high-redox potential oxidant or a low-redox potential reductant, a catalytic module that uses the hole or the electron to carry out oxidative or reductive chemistry, respectively, and a method for transferring electrons efficiently between the two modules. The design philosophy described here is to employ isolated components rather than living cells and to separate the necessary reactions into photoelectrochemical anodic and cathodic half-cell modules. In this work, we will focus exclusively on the cathodic half-cell, in which the reaction $2H^+ + 2e^- \rightarrow H_2$ is carried out at the expense of light.

PHOTOCHEMICAL MODULE

All photochemical systems, whether type I and type II reaction centers from natural photosynthetic organisms (*1*) or silicon-based, artificial photovoltaic cells, function by producing a charge-separated state upon the absorption of a photon. In photovoltaic devices, the electron and hole diffuse quickly within the conduction and valence bands from the initial site of charge separation, ultimately generating an electrical current that must be used in real time. Very little recombination occurs between the electron and the hole. Instead, inefficiencies arise from trapping of the mobile carriers as a result of defects, such as dangling bonds in grain boundaries within polycrystalline materials. In the photosystems of biological organisms, an electron and a hole are similarly formed, but a crucial difference is that they are tightly confined to molecular orbitals within closely spaced donor and acceptor molecules. As a result, the charge-separated state is immediately susceptible to charge recombination, with the consequence that the electron must rapidly be transported to a more distant secondary acceptor to extend the lifetime of the charge-separated state.

An ideal photochemical module would have the following attributes. (i) Light-induced charge separation should be highly efficient; i.e., each absorbed photon should lead to one electron–hole pair. (ii) The resulting charge-separated state should have a sufficiently long lifetime that forward electron transfer to the catalytic module will outcompete charge recombination. (iii) The maximum amount of energy in the photon should be utilized to carry out the catalytic event rather than be lost in stabilizing a
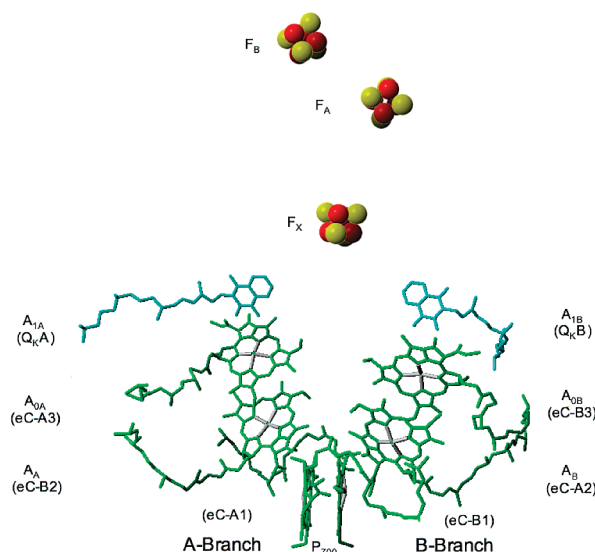

FIGURE 1: Arrangement of the electron transfer cofactors in PS I from *T. elongatus*. The C_2 axis of symmetry occurs between the center of P_{700} and the F_X cluster. The spectroscopic names of the cofactors are depicted (the crystallographic names are in parentheses). The chlorophyll molecules are colored green, the phylloquinones yellow, and the iron−sulfur clusters red/yellow, where red is iron and yellow is sulfur (PDB entry 1JB0).

longer-than-necessary charge-separated state. (iv) An antenna system should be present so that the photochemical module will be able to deliver a maximal or optimal number of electrons per unit time to the catalytic module. (v) The photochemical module should be robust or self-repairing when operating under (nearly) continuous light. Although there have been impressive gains in the area of artificial photosynthesis, at present there are no human-engineered systems that fulfill all (or even most) of these design criteria. In contrast, through the processes of evolution and natural selection over the course of 3.5 Ga, the PS I reaction centers of cyanobacteria and plants have achieved all of these attributes (*2−5*).

The PS I reaction center from the cyanobacterium *Thermosynechococcus elongatus* has been crystallized, and its structure has been determined to a resolution of 2.5 Å (*6*). Figure 1 depicts the arrangement of the electron transfer cofactors in this integral membrane protein. Light is absorbed by one of 90 accessory chlorophyll *a* molecules and 22 β-carotenes that serve as the antenna (not depicted). The excited state migrates to the six core chlorophylls shown, whereupon charge separation occurs between the eC-A1/eC-B1 special pair, named P_{700}, and the primary acceptor (either eC-A3 or eC-B3), named A_{0A} or A_{0B}. The electron is subsequently transferred to a bound phylloquinone (Q$_K$A or Q$_K$B) and then serially through three [4Fe-4S] clusters, F_X, F_A, and F_B, to a soluble, oxygen-stable [2Fe-2S] ferredoxin (not shown). Figure 2 depicts the electron transfer kinetics as well as the midpoint potentials of the cofactors (ordinate) and distance in the membrane normal (abscissa) on the two branches of electron transfer cofactors. The design principle, upon which all photochemical reaction centers are based, is to use a portion of the energy from the absorbed photon to increase the distance between the charge-separated radical pair. This decreases the probability and thus reduces the rate of the nonproductive back-reaction (*7, 8*). As an example, the charge-separated state between P_{700}^+ and A_{0A}^- (or P_{700}^+ and A_{0B}^-) has an inherent lifetime of 10 ns, but this reaction does not occur to a significant extent because the electron is transferred forward to A_{1A}^- (or A_{1B}^-)
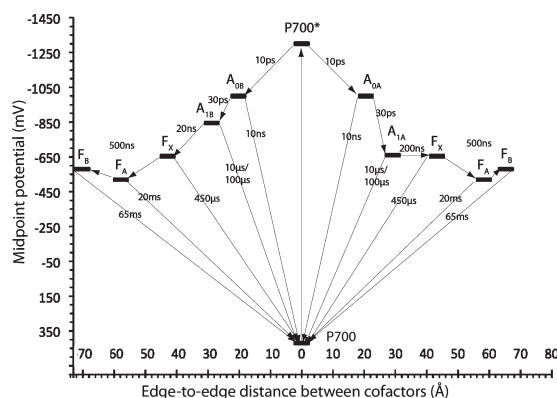
FIGURE 2: Forward and backward electron transfer kinetics, as well as the redox potentials (ordinate) and distance in the membrane normal (abscissa) on the A branch (right) and B branch (left) of the electron cofactors in PS I. Since the electron transfer pathways converge at F_X, the left and right sides represent identical clusters, F_X, F_A, and F_B.

with a much faster time constant of ~50 ps. With each electron transfer step, additional distance, and hence lifetime, is purchased at the expense of a portion of the Gibbs free energy of the initial photon. The ultimate charge-separated state between P_{700}^+ and F_B^- has a lifetime of 60 ms, which is sufficiently slow to allow diffusion-limited, solution chemistry events to outcompete the back-reaction and other nonproductive reactions.

PHOTOSYSTEM I AS THE PHOTOCHEMICAL MODULE

PS I has a number of favorable properties for application as the photochemical module.

(*i*) *The Pigments in PS I Absorb All Wavelengths Shorter Than 700 nm.* This region represents 43−46% of the total solar emission that reaches the surface of the Earth at aphelion and perihelion (*9, 10*). The absorption in the blue and red regions by the 96 chlorophyll *a* and 22 β-carotene molecules is especially notable, and at high pigment concentrations, total absorption for $\lambda < 700$ nm is readily approached.

(*ii*) *The Antenna Chlorophylls in PS I Provide a Large Optical Cross Section.* Given the area of one chlorophyll *a* molecule and a noon solar flux at the latitude of Washington, DC, in summer, full sunlight excites each chlorophyll *a* in PS I 10 times per second. Because there are nearly 100 chlorophyll molecules per P_{700} in each PS I reaction center, up to 1000 photons can be absorbed per second. Thus, if all of the nonphotochemical reactions can be completed in less than 1 ms, at least 1000 electrons can be processed per second per reaction center in full sunlight.

(*iii*) *The Quantum Yield of PS I Approaches 1.0.* Regardless of its wavelength, every absorbed photon generates the charge-separated $P_{700}^+F_B^-$ state.

(*iv*) *The Thermodynamic Efficiency of Charge Separation Is High.* The 1.01 V of Gibbs free energy stored in the charge-separated $P_{700}^+F_B^-$ state represents a remarkable 59% conversion efficiency for a red photon and a respectable 38% conversion efficiency for a blue photon (*11, 12*).

(*v*) *The Lifetime of the Charge-Separated State Is Long.* The charge-separated $P_{700}^+F_B^-$ state has a lifetime of 60 ms, which is sufficient time to capture the electron to perform useful work.

(*vi*) *PS I Delivers Electrons at a Redox Potential Sufficiently Low To Drive H_2 Evolution.* The F_B cluster has a pH-independent redox potential of −580 mV (*11, 12*), which is 166 mV

more reducing than the half-cell potential for the H^+/H_2 couple: $2H^+ + 2e^- \leftrightarrow H_2$ at pH 7.0. Thus, the reduction of $2H^+$ to H_2 is thermodynamically favorable, with sufficient electromotive force to drive the reaction to (near) completion.

(*vii*) *The PS I Reaction Center Is Robust.* There are no overly light or heat sensitive components in PS I. The only reported form of damage is a chilling-induced (4 °C) photoinhibition, which has been described in leaves (*13*) and membranes (*14*) of some cold-sensitive plants and which results in destruction of the Fe−S clusters. The causative agent is the •OH radical, formed in the presence of H_2O_2 by the reduced Fe−S clusters of PS I (*15*). Because the photochemical half-cell described below functions under anoxic conditions, this mode of damage should not occur.

(*viii*) *The Cofactors and Proteins That Constitute PS I Can Be Readily Manipulated.* Over the past 20 years, methods have been pioneered for (i) the biochemical removal (*16−18*) and reconstitution (*18−20*) of PS I with recombinant PsaC, PsaD, and PsaE proteins (*21−23*), (ii) the chemical removal and reinsertion of the F_X, F_A, and F_B clusters (*24−27*), and (iii) the selective removal (*28, 29*) and the site-directed mutagenesis of the proteins that constitute PS I (reviewed in ref *30*).

CATALYTIC MODULE

The reduction of protons to H_2 is a deceptively simple yet inherently difficult reaction: $2H^+ + 2e^- \leftrightarrow H_2$. This reaction can be conducted by employing metal catalysts such as gold, platinum, osmium, and ruthenium. Noble metals such as platinum are able to carry out the reduction of protons to H_2 near the thermodynamic midpoint potential, i.e., without a significant overpotential. Briefly, two hydrogen ions are adsorbed to the metal surface and become reduced to form $H_{(ads)}$. Two equivalents of $H_{(ads)}$ combine to generate $H_{2(ads)}$, which then desorbs from the metal surface to produce $H_{2(g)}$. Photocatalytic H_2 production is possible by using semiconductor-supported metal catalysts. In this situation, the semiconductor absorbs a photon and, if the photon has the appropriate energy to span the band gap, creates an electron−hole pair, which supplies the reducing power necessary to reduce protons adsorbed to the metal surface. Titania [titanium(IV) dioxide] is frequently used as the semiconductor; however, titania requires photons with energies of ≥3.2 eV (shorter than 360 nm) to span the band gap. The high-energy photons that meet this requirement comprise only a tiny fraction of the solar energy that reaches the Earth's surface, and the low overall efficiency of semiconductor-based, photocatalytic H_2 production may ultimately limit further development of this technology.

HYDROGENASE AS THE CATALYTIC MODULE

Microorganisms have evolved a class of enzymes, termed hydrogenases, that also carry out the reversible reaction: $2H^+ + 2e^- \leftrightarrow H_2$. Like the noble metals, these naturally occurring, biological catalysts are also able to reduce protons to H_2 while operating near the thermodynamic midpoint potential. Three chemically distinct and evolutionarily unrelated classes of H_2ases are known: (i) [Hmd]-H_2ases, (ii) [NiFe]-H_2ases, and (iii) [FeFe]-H_2ases. Thauer and co-workers discovered the [Hmd]-H_2ase in methanogens (*31*). This enzyme, which acts as a H_2-forming methylenetetrahydromethanopterin dehydrogenase (Hmd), lacks Fe−S clusters but contains a single Fe atom with two CO ligands at its active site (*32−34*). The [Hmd]-H_2ase is light-sensitive and thus is not useful for solar H_2 production; therefore, it will not be discussed further here (*35*).

High-resolution X-ray structures of the [FeFe]-H$_2$ase (Figure 3A) and [NiFe]-H$_2$ase (Figure 3B) enzymes have revealed that these enzymes are structurally distinct, convergently evolved metalloproteins that catalyze the same reaction using very different active site metal centers (*36*). Microorganisms often use [NiFe]-H$_2$ases, which are usually less sensitive to inactivation by oxygen, for H$_2$ oxidation. [FeFe]-H$_2$ases, which are rapidly and irreversibly inactivated by oxygen, commonly occur in microorganisms that produce H$_2$ during fermentation or anaerobic respiration. Both H$_2$ase classes have a dimetal active site with CO and CN ligands, and both enzyme classes usually include multiple Fe–S clusters that participate in electron transfer reactions between the active site and the electron donor or acceptor molecules that interact with the surface of the enzyme. Four [4Fe-4S] clusters and one [2Fe-2S] cluster occur in the [FeFe]-H$_2$ase of *Clostridium pasteurianum* shown in Figure 3A. One of the [4Fe-4S] clusters is covalently linked to the proximal Fe atom of the H-cluster at the active site through the sulfur atom of a bridging Cys residue.

[NiFe]-H$_2$ases comprise the largest and best-studied H$_2$ase family, and examples are known from organisms belonging to bacteria and archaea. All of these enzymes have a heterodimeric core comprising a large, ~60 kDa subunit and a smaller, ~30 kDa subunit (Figure 3B) (*37, 38*). The bimetallic active site is associated with the larger subunit and is deeply buried near the interface with the smaller subunit. The sulfur atoms of four cysteinates, two of which are bridging ligands to the Fe atom, coordinate the Ni atom. In some enzymes of this class, one of the cysteine ligands is replaced by selenocysteine. The Fe atom at the active site typically has two CN ligands and one CO ligand. Gas channels that allow H$_2$ to diffuse into or out of the active site have been identified (*36*). Three Fe–S clusters on the small subunit connect the buried [NiFe] active site with electron donors and acceptors at the surface of the enzyme. In most [NiFe]-H$_2$ases, the medial Fe–S cluster is a [3Fe-4S] cluster, but in some [NiFe]-H$_2$ases, all three Fe–S clusters are [4Fe-4S] clusters. The metal insertion and maturation processes of [NiFe]-H$_2$ases are complex and require the participation of at least seven accessory proteins (for reviews, see refs *36, 39,* and *40*).

[FeFe]-H$_2$ases are often monomeric enzymes that are widely distributed in anaerobic members of the domain of bacteria, including clostridia and sulfate-reducing bacteria, and they represent the only type of H$_2$ase that has been found in members of the domain eukarya. These enzymes are remarkable catalysts and can accept electrons from, or donate electrons to, many different physiological electron carriers. Under optimal conditions at 30 °C, the [FeFe]-H$_2$ase of *C. pasteurianum* can produce ~6000 molecules of H$_2$ per second. The most simple [FeFe]-H$_2$ases occur in green algae such as *Chlamydomonas reinhardtii* (*41, 42*); these enzymes contain a binding site for the H-cluster but lack peripheral Fe–S clusters. The X-ray crystal structure for the *C. pasteurianum* [FeFe]-H$_2$ase (Figure 3A) reveals a mushroom-shaped protein, in which the H-cluster is deeply buried within the protein. The H-cluster comprises a binuclear Fe–Fe center bound by a bridging cysteine to a [4Fe-4S] cluster, which is bound to the protein through three additional Cys ligands. CO and CN ligands are associated with each Fe atom of the binuclear center. The two Fe atoms of the binuclear H-cluster are also bridged by a small molecule, which was originally suggested to be 1,3-propanedithiol but which is now thought to be
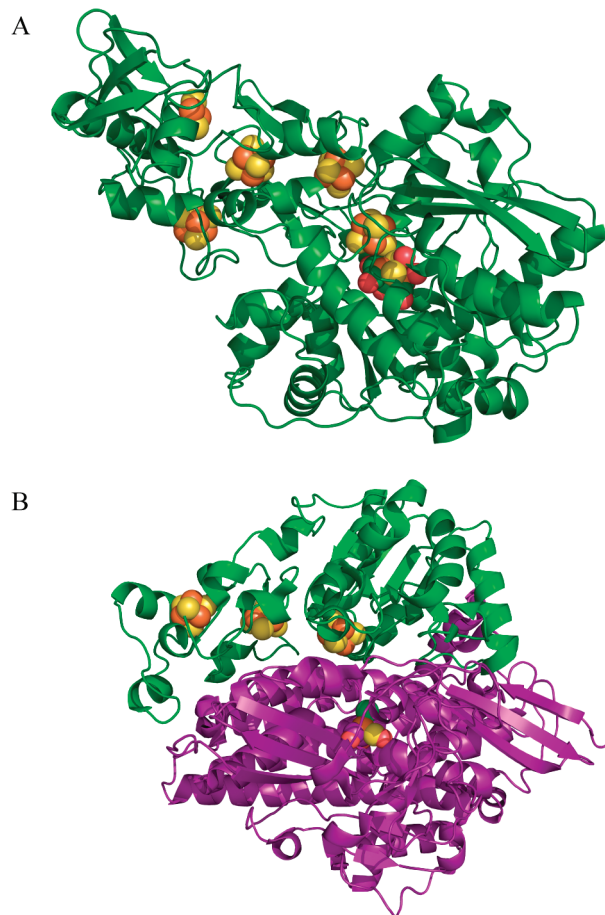
FIGURE 3: X-ray crystal structure of the [FeFe]-H$_2$ase from *C. pasteurianum* (PDB entry 1FEH) (A) and the [NiFe]-H$_2$ase from *Desulfovibrio gigas* (PDB entry 1FRV) (B).

di(thiomethyl)amine (*43*). The metal insertion and maturation properties of [FeFe]-H$_2$ases are also complex; however, the fully formed active enzyme has been isolated from *Escherichia coli* with the additional expression of the *hydEFG* maturation genes (*44*).

For either type of H$_2$ase to be useful as the catalytic module of devices for H$_2$ production, one must be able to produce variant forms of these enzymes that can be coupled to the photochemical module. The use of a molecular wire to perform this coupling requires that a Cys ligand to a surface-located [4Fe-4S] cluster of the H$_2$ase be converted to a Gly residue and that an active H$_2$ase can still be assembled. However, the ability to manipulate H$_2$ases has not yet advanced to the same stage as for PS I, although there are reasons to believe that this may soon be the case. For example, *Ralstonia eutropha* mutants lacking the small subunit of [NiFe]-H$_2$ase can assemble mature, large subunits, and conversely, mutants lacking the large subunit can assemble mature, small subunits, which contain the distal, medial, and proximal Fe–S clusters (*45*). In the case of [FeFe]-H$_2$ase from *Clostridium acetobutylicum*, heterologous expression of a variant form of HydA in which Cys$_{97}$ was replaced with glycine led to the production of active H$_2$ase when this variant was coexpressed with the crucial maturation genes in *E. coli* (P. Silva, J. H. Golbeck, and D. A. Bryant, unpublished results). As described below, this H$_2$ase variant can be coupled to the photochemical module, and the resulting complex produces H$_2$ when it is illuminated in the presence of a sacrificial electron donor to PS I.

PLATINIZED PHOTOSYSTEM I

Greenbaum and co-workers pioneered the direct attachment of a catalyst, metallic platinum, to the PS I complex. The Hill reaction of photosynthesis, which reduces ferric ions to ferrous ions, forms the basis for the photoprecipitation of metallic platinum onto the external surfaces of spinach thylakoid membranes and isolated PS I complexes (*46−48*). When hexachloroplatinate ($[PtCl_6]^{2-}$) is added to a solution containing spinach chloroplasts and the solution is illuminated, the Pt ion is reduced to Pt(s) in a four-electron process. Once the Pt has precipitated onto PS I, continued illumination enables H_2 production. Maximum rates of light-generated H_2 production were observed in colloidal deposits that averaged between 50 and 500 Pt atoms (*47*). Hexachloroosmiate ($[OsCl_6]^{2-}$) can also be photoprecipitated onto chloroplasts, and such precipitates are capable of photocatalytic H_2 evolution [0.113 μmol of H_2 (mg of Chl)$^{-1}$ h^{-1}] at rates faster than those for platinized chloroplasts (*48*). Additionally, hexachlororuthenate $[RuCl_6]^{2-}$ can be photoprecipitated onto chloroplasts alone or in combination with $[PtCl_6]^{2-}$ and is also capable of photocatalytic H_2 evolution, albeit at lower rates (*49*).

Isolated PS I protein complexes also have the ability to evolve H_2 after photoprecipitation of Pt (*50*). Plastocyanin was required for rapid photoreduction of $[PtCl_6]^{2-}$ as well as for light-induced H_2 evolution [0.025 μmol of H_2 (mg of Chl)$^{-1}$ h^{-1}]. After plastocyanin was cross-linked to spinach PS I and the resulting complexes were platinized, subsequent illumination led to H_2 production at a rate 3-fold higher than that of PS I complexes to which plastocyanin had not been cross-linked [~0.080 μmol of H_2 (mg of Chl)$^{-1}$ h^{-1}] (*51*).

PHOTOSYSTEM I−HYDROGENASE FUSION COMPLEXES

One approach to connecting PS I and H_2ase is to generate a fusion protein with the hope that the F_B cluster of PS I and the distal Fe−S cluster of H_2ase are sufficiently close that forward electron transfer outcompetes charge recombination. A hybrid complex, consisting of a [NiFe]-H_2ase and cyanobacterial PS I, was constructed by fusing the H_2ase with the small stromal protein, PsaE, of PS I (*52*). The oxygen-tolerant, membrane-bound [NiFe]-H_2ase from *R. eutropha* is composed of two subunits, the smaller HoxK subunit and the larger HoxG subunit (*53*). To generate a fusion protein with PS I, the membrane anchor domain of HoxK was substituted with a linker peptide (Ser-Gly-Gly), which was in turn fused to a His$_6$-tagged variant of PsaE from *T. elongatus*. The HoxK-PsaE-His$_6$ fusion protein associates with HoxG in vivo, resulting in a functional H_2ase−PsaE complex. The purified H_2ase−PsaE fusion complex produced 0.0072 μmol of H_2 (mg of protein)$^{-1}$ h^{-1}, which corresponds to 16% of the activity of the wild-type H_2ase enzyme. When PS I complexes from a PsaE-less cyanobacterial mutant were combined with this H_2ase−PsaE fusion protein, the two complexes spontaneously associated to produce a H_2ase−PS I complex that could be isolated by sucrose density gradient centrifugation. To prove that the H_2ase was bound to PS I through the PsaE fusion, excess PsaE was added to displace the H_2ase−PsaE fusion competitively, which could be assayed by the loss of H_2 evolution activity. When illuminated, the complete system supported H_2 production with a maximal rate of 0.58 μmol of H_2 (mg of Chl)$^{-1}$ h^{-1}. Although the aim of this design was to bring H_2ase into the proximity of the terminal

Fe−S clusters of PS I, which on the basis of the X-ray crystal structures were estimated to be separated by only 14 Å, the rate of H_2 evolution was much lower than expected. The rate-limiting step in this system appears to be the transfer of electrons between the photochemical and catalytic modules, as this step is dependent on the relative motion of the two enzymes. The probability that the two Fe−S clusters will be at a distance and orientation for rapid electron transfer at any given time is likely to be low. Overcoming this rate limitation remains a major concern for any system that intends to produce light-induced H_2 using photosynthetic complexes.

CONNECTING PHOTOCHEMISTRY AND CATALYST

A major challenge for systems that aim to produce light-induced H_2 is to devise a more direct method to transfer electrons from the photochemical module to the catalytic module. The specific issue in the case of PS I is how to transfer the electrons from the terminal, F_B, cluster to the catalytic module at a rate faster than the lifetime of the charge-separated $P_{700}^+F_B^-$ state. In living cells, the coupling is carried out by freely diffusible proteins, e.g., ferredoxin, which accepts an electron from F_B and donates it to redox partners such as ferredoxin:NADP$^+$ oxidoreductase or nitrate reductase. The relatively high concentrations of such proteins and the short distances between donor−acceptor protein partners in living cells make diffusion chemistry a realistic option, which can lead to electron transfer within the lifetime of the charge-separated state. In an in vitro device, the distances between the photochemical and catalytic modules are usually much greater and a different strategy for electron transfer is needed.

QUINONE EXCHANGE REACTIONS

The native phylloquinone present in the A_{1A} and A_{1B} sites can be extracted from plant and cyanobacterial PS I using 50% diethyl ether in water, leaving empty A_{1A} and A_{1B} sites and a PS I complex that has severely inhibited photoactivity beyond A_{0A} and A_{0B} (*54*). It is then possible to wire PS I in such a way that an electron transfer chain is extended out of the membrane from A_{1A} and A_{1B} sites to a redox dye (*55*), to a gold nanoparticle, or to an electrode (*56*). In refs *55* and *56*, a quinone-free PS I complex was generated using PS I from *T. elongatus*. A molecular wire consisting of a naphthoquinone connected through an alkyl chain linker to a viologen compound was adsorbed to a gold electrode. The electrode containing the modified quinone was immersed in quinone-free PS I, thus reconstituting the A_{1A} and A_{1B} sites and consequently wiring PS I to the electrode surface. The naphthoquinone acts to rescue the empty A_{1A} and A_{1B} sites, while the viologen acts as an electron transfer cofactor. The alkyl linker ensures that the viologen remains at an appropriate distance outside of the PS I core. Transient absorption measurements at 600 nm were performed to assess if the viologen becomes reduced. A broad peak was produced upon photoexcitation at 440 nm for the wired PS I construct and was not seen for wild-type PS I.

When this quinone-free PS I was reconstituted with a wire that contained a gold nanoparticle in place of the viologen unit, photo-oxidation of P700 was observed, confirming the ability to reconstitute the A_{1A} and A_{1B} sites and form a fully active PS I complex. Because PS I contains two phylloquinone binding sites, two gold nanoparticles could potentially be tethered to a single
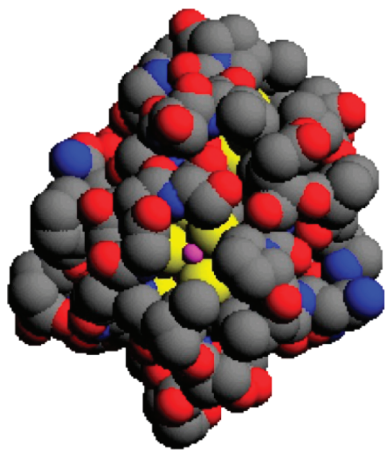
FIGURE 4: Depiction of exposed iron atom in the $Cys_{13}Gly$ variant of unbound PsaC in the absence of 2-mercaptoethanol. The surface accessibility of one of the cubane iron atoms is clearly seen in this CPK depiction (PDB entry 1JB0).

PS I complex, as was seen in TEM images. The gold nanoparticle-tethered PS I construct was then adsorbed to a gold electrode through Au−S bonds, and the construct's photoactivity remained intact. It is possible that this highly tailorable technology could be adapted for attachment of PS I to a catalytic module.

Direct coupling of the photochemical and catalytic modules is an alternative approach for the construction of a light-driven, H_2-evolving device. To transfer electrons efficiently and with a high quantum yield, we conceived and have employed a molecular wire that covalently attaches the F_B cluster of PS I to either a Pt nanoparticle or the distal Fe−S cluster of H_2ase.

ATTACHMENT OF AN EXTERNAL LIGAND TO THE F_B CLUSTER OF PSAC

The concept for a covalently bound molecular wire was derived from studies of PsaC variants with modified cysteine ligands to the F_B cluster. Because the literature is scant on the topic of rescue ligands to Fe−S clusters, a brief description of how this idea came about is warranted. Two methods were used to generate mutants affecting PS I. In the first, so-called in vivo approach, mutagenesis of PsaC was conducted within the cyanobacterium *Synechocystis* sp. PCC 6803 by gene replacement through homologous recombination (*57, 58*); in the second, so-called in vitro approach, recombinant variants of PsaC were produced in *E. coli*, after which the PsaC apoproteins were purified, reconstituted with two [4Fe-4S] clusters, and re-bound to P700-F_X cores in the presence of PsaD to rebuild functional PS I complexes (*23, 59−63*).

In the in vivo approach, the cellular machinery inserts the [4Fe-4S] clusters into PsaC. It was found that when the second cysteine (Cys_{13}) of the $CxxC_{13}xxCxxxCP$ motif was changed to Asp and Ser, a [4Fe-4S] cluster formed in the F_B site, but when the second cysteine was changed to Gly, no PS I complexes accumulated in the cyanobacterial cells (*57, 58*). Because two [4Fe-4S] clusters were present in the Asp and Ser mutants, the side chain oxygen of these amino acids serves as a ligand to the iron in the differentiated site. However, when no side chain is present as in the Gly mutant (Figure 4), the [4Fe-4S] cluster either does not initially form or the cell recognition machinery identifies the cluster as damaged and targets the entire PS I complex for degradation.

In the corresponding in vitro studies, PsaC variants were expressed in *E. coli* as apoproteins in the form of inclusion bodies, and the [4Fe-4S] clusters were inserted by the addition of a ferrous salt together with sodium sulfide and 2-mercaptoethanol. The mechanism of the cluster insertion is not known with certainty. However, it is assumed that inorganic [4Fe-4S]·$(S-(CH_2)_2-OH)_4$ clusters are preformed, and that through a ligand exchange reaction, the [4Fe-4S] clusters are exchanged into the protein by displacement of the 2-mercaptoethanol ligands by the sulfhydryl side chains of the cysteine residues in PsaC. Given the similarity in the Fe−S coordination bond between the cysteine and 2-mercaptoethanol, the enthalpic contribution to the free energy of cluster insertion is likely to be negligible. Because of the statistics of converting one PsaC apoprotein and two [4Fe-4S]·$(S-(CH_2)_2-OH)_4$ clusters into one PsaC holoprotein and eight 2-mercaptoethanol molecules, the entropic contribution to the free energy change drives the reaction to completion. Importantly, when the second cysteine of the $CxxC_{13}xxCxxxCP$ motif is changed to Gly as well as Asp and Ser, a [4Fe-4S] cluster is formed in the F_B site (*59, 64*).

Why is a [4Fe-4S] cluster present in the Gly variant in vitro but not in the Gly variant in vivo? Because Gly has no side chain, a reasonable assumption is that one 2-mercaptoethanol molecule is retained as an Fe−S ligand, resulting in a [4Fe-4S]·$(Cys)_3$-$(S-(CH_2)_2-OH)$ cluster in the F_B site (Figure 5). The mechanism of biological insertion must be sufficiently different from the in vitro cluster exchange mechanism described above that no rescue ligand follows the cluster into the protein. This might be expected if the Fe−S cluster were exchanged into PsaC from a scaffold protein such as NfuA (*65*), because the Cys ligands in the scaffold protein would not be free to migrate into the acceptor protein. Under these conditions, the empty coordination site (see Figure 4) or incomplete cluster transfer likely destabilizes the [4Fe-4S] cluster, and this targets the protein for turnover. The presence of an external ligand in the differentiated site of the in vitro PsaC variant was proven when p-F^{19}-benzenethiol was used to generate synthetic [4Fe-4S]·$(S-(C_6H_4)-F)_4$ clusters. The NMR chemical shift and paramagnetic broadening of the F^{19} prove that the thiol group from $HS-C_6H_4-F$ functions as the ligand in the differentiated site of reconstituted PsaC (*64*). One interesting detail is that the ground spin state (S) of the [4Fe-4S]·$(Cys)_3(S-(CH_2)_2-OH)$ cluster in the F_B site is $\geq \frac{3}{2}$, whereas the ground spin state (S) of the [4Fe-4S]·$(Cys)_4$ cluster in the F_A site remains $\frac{1}{2}$. The spin state serves as a convenient spectroscopic marker for the F_A and F_B clusters in the $Cys_{13}Gly$ variant of PsaC.

In essence, 2-mercaptoethanol functions as a "rescue ligand" for the [4Fe-4S] cluster in the differentiated site that involves the Gly residue (*64*). In principle, two methods are available to attach different ligands to the F_B cluster of the $Cys_{13}Gly$ variant of PsaC. One is to synthesize [4Fe-4S]·$(SR)_4$ clusters, in which R is the desired thiolate. The product is a protein-bound [4Fe-4S]·$(Cys)_3(SR)$ cluster. Another method is to synthesize a [4Fe-4S]·$(S-(CH_2)_2-OH)_4$ cluster, carry out the insertion of the the cluster into the PsaC variant, and subsequently displace the single 2-mercaptoethanol rescue ligand on the PsaC-bound [4Fe-4S]·$(Cys)_3(S-(CH_2)_2-OH)$ cluster with the desired thiolate (Figure 5). Que and Holm (*66*) showed facile thiol displacement reactions in synthetic tetranuclear clusters of the type $[Fe_4S_4(SR)_4]^{2-}$ (R = alkyl, aryl), which are closely related to the active sites in oxidized ferredoxin proteins. Ligand exchange reactions occur in
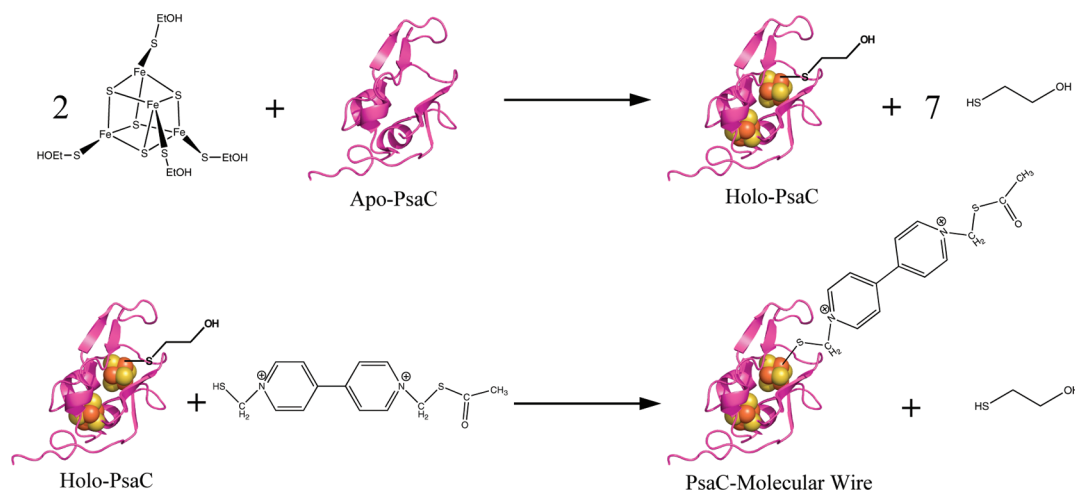
FIGURE 5: Proposed method of insertion of a cluster into the $Cys_{13}Gly$ variant of unbound PsaC (top) and displacement of the 2-mercaptoethanol rescue ligand with an external thiolate (bottom). The external ligand is 1-(3-thiopropyl)-1′-[3-(acetylthio)propyl]-4,4′-bipyridinium. For the sake of clarity, the molecular wire is not scaled to the same dimension as the protein.

nonaqueous media without any significant degradation of the cubane core and with substitution affinities that roughly parallel the pK_a values down to a pK_a of ≤6.5. Similar exchange reactions are expected to occur with the external rescue ligand to the $Cys_{13}Gly$ variant of PsaC. In practice, both methods appear to be equally effective at introducing a foreign rescue ligand in the differentiated Fe−S site of PsaC.

PHOTOSYSTEM I−DIPYRIDINIUM TETHER

The next question is whether it is possible to use a molecular wire to transfer electrons from PS I to a catalytic module. To test the effectiveness of a wire, a viologen derivative, 1-(3-thiopropyl)-1′-[3-(acetylthio)propyl]-4,4′-bipyridinium, was synthesized and attached to the differentiated site of the $Cys_{13}Gly$ variant of PsaC by exchange of the 2-mercaptoethanol ligand in the [4Fe-4S]·$(Cys)_3(S-(CH_2)_2-OH)$ cluster, producing a [4Fe-4S]·$(Cys)_3$(1-(3-thiopropyl)-1′-[3-(acetylthio)propyl]-4,4′-bipyridinium) cluster (Figure 5). The midpoint potential of the synthesized bipyridinium is similar to that of paraquat ($E'° = -440$ mV), and therefore electron transfer from F_B ($E'° = -580$ mV) to the dye is thermodynamically favorable. When the reconstituted PsaC variant was purified and then reduced with sodium hydrosulfite, the low-temperature EPR spectrum showed a broad, axial set of resonances due to $S = {}^1/_2$ [4Fe-4S] in the F_A site, and a sharp, derivative resonance due to the $S = {}^1/_2$ bipyridinium radical. This indicated that the bipyridinium derivative was an integral part of the variant PsaC protein. The reconstituted PsaC variant was then bound to P700-F_X cores in the presence of PsaD. By measurement of the light-induced, steady-state kinetics for the absorption increase at 600 nm of the wired PS I construct, a rate of 58.3 μmol of bipyridinium radical (mg of Chl)$^{-1}$ h^{-1} was achieved using soluble Cyt c_6 as a mediator and ascorbate as the sacrificial electron donor to $P_{700}{}^+$ (C. E. Lubner, D. A. Bryant, and J. H. Golbeck, unpublished results). Furthermore, the absorbance at 600 nm reached a maximum and then subsequently decreased over time as more electrons entered into the wire, which is consistent with the production of doubly reduced bipyridinium. This proof of principle opened the door to the construction of a photochemical module that could be directly wired (i.e., covalently attached) to a variety of catalytic modules, for example, gold and platinum nanoparticles, H_2ase, or other types of biological or inorganic catalysts.
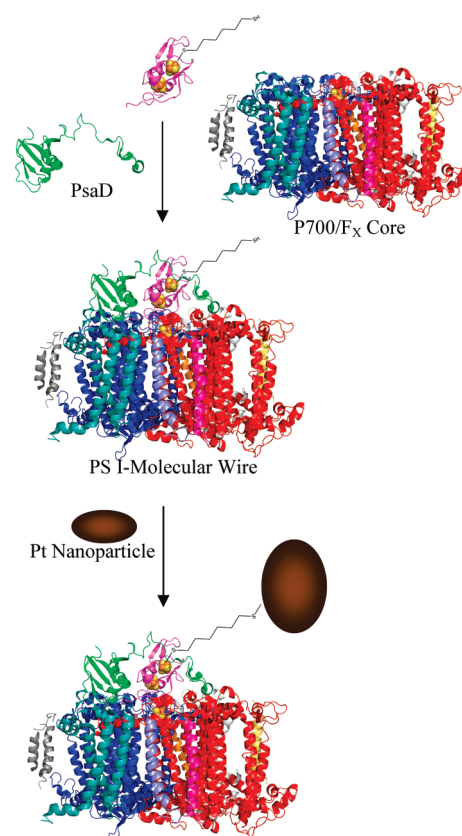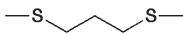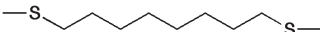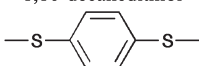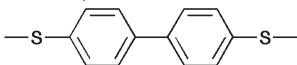

FIGURE 6: Stepwise assembly of the PS I−molecular wire−Pt nanoparticle bioconjugate beginning with the Fe−S reconstituted $Cys_{13}Gly$ variant of unbound PsaC. The molecular wire is 1,6-hexanedithiol. For the sake of clarity, the molecular wire and Pt nanoparticle are not scaled to the same dimension as the protein.

PHOTOSYSTEM I−MOLECULAR WIRE−NANO-PARTICLE BIOCONJUGATES

In the same way that 1-(3-thiopropyl)-1′-[3-(acetylthio)propyl]-4,4′-bipyridinium is capable of displacing the 2-mercaptoethanol molecule that occupies the differentiated site of the F_B cluster in the $Cys_{13}Gly$ variant of PsaC, alkyl and aryl dithiol linkers are also capable of displacing the rescue ligand. The formation of PS I−dithiol molecular wire−nanoparticle bioconjugates exploits this ability by allowing one sulfhydryl group of the

Table 1: Molecular Wire Lengths and Bond Saturation Affect the Rate of Production of H$_2$ by Plastocyanin Cross-Linked Rebuilt Spinach PS I−Dithiol Molecular Wire−Pt Nanoparticle Bioconjugates[a]

Molecular wire	Rate of H$_2$ production (μmol H$_2$ mg Chl^{-1} h^{-1})	Rate of H$_2$ production (mol H$_2$ mol PS I^{-1} s^{-1})
—S‿‿S— 1,3-propanedithiol	2.5	0.09
—S‿‿‿‿S— 1,6-hexanedithiol	98.6	3.52
—S‿‿‿‿‿S— 1,8-octanedithiol	49.0	1.75
—S‿‿‿‿‿‿S— 1,10-decanedithiol	16.1	0.57
—S⬡S— 1,4-benzenedithiol	150.5	5.37
—S⬡⬡S— 4,4'-biphenyldithiol	92.5	3.31

[a]From ref *68*. Copyright 2009. Royal Society of Chemistry.

dithiol molecule to displace the 2-mercaptoethanol molecule and permitting the other sulfhydryl group of the dithiol to functionalize a Au or Pt nanoparticle surface (Figure 6). This approach is highly tailorable and directly links an electron transfer cofactor, the F$_B$ [4Fe-4S] cluster of PS I, with the catalytic surface of a Au or Pt nanoparticle.

The PS I−molecular wire−nanoparticle bioconjugates form spontaneously when cyanobacterial PS I complexes that have been rebuilt with the Cys$_{13}$Gly variant of PsaC are combined by using dithiol linkers with 3 nm Pt nanoparticles or 12 nm Au nanoparticles (*67*). With sodium ascorbate as the sacrificial donor and 2,6-dichlorophenolindophenol (DPIP) as the mediator, illumination of the bioconjugates with white light generated H$_2$ initially at rates of 3.4 μmol of H$_2$ (mg of Chl)$^{-1}$ h^{-1} for Au nanoparticle bioconjugates and 9.6 μmol of H$_2$ (mg of Chl)$^{-1}$ h^{-1} for Pt nanoparticle bioconjugates. When wild-type (unmodified) PS I was used, or when any one of the components was eliminated, no H$_2$ production was observed. The addition of Cyt c_6, the native electron donor to P$_{700}^+$ of PS I in cyanobacteria, increased the rate of H$_2$ production by Pt nanoparticle bioconjugates approximately 5-fold. This increase implied that the rate limitation in H$_2$ production was due to the diffusion of electron-donating species to P$_{700}^+$.

As discussed earlier, cross-linking of plastocyanin to PS I led to an increase in the rate of light-induced H$_2$ generation in platinized spinach PS I particles (*51*). Therefore, plastocyanin isolated from spinach leaves was cross-linked to spinach PS I core complexes that had been rebuilt using the Cys$_{13}$Gly variant of PsaC. Bioconjugates constructed from these plastocyanin cross-linked, spinach PS I complexes evolved H$_2$ at twice the rate of bioconjugates mixed with soluble plastocyanin (*68*). Plastocyanin can be more efficiently cross-linked to spinach PS I complexes than Cyt c_6 can be cross-linked to cyanobacterial PS I complexes.

Lowering the pH of the buffer to 6.0 increases the rate of production of H$_2$, possibly due to a higher concentration of the H$^+$ ions at the nanoparticle surface. However, the bioconjugates are susceptible to irreversible aggregation at pH < 6.0 and at high ionic strengths (> 25 mM MgCl$_2$) (*68*). Changing the dithiol linker between PS I and the Pt nanoparticle also altered the rate

of H$_2$ production (Table 1). Very short molecular wires resulted in low rates of light-induced H$_2$ generation, either due to inefficient coupling or to an inability to shield the protein from denaturation by the metal surface of the Pt nanoparticle. Aliphatic dithiol wires longer than six carbon atoms also resulted in lower rates of H$_2$ production, while the use of aromatic dithiol molecular wires resulted in the best rates of H$_2$ production. Although the relationship between wire length and chemical properties is not yet completely understood, one possibility is that the efficiency of the formation of the Pt bioconjugates fluctuates for the differing molecular wires. Another possibility is that forward electron transfer is sufficiently slow through the wire that with increasing length, forward electron transfer no longer outcompetes charge recombination between P$_{700}^+$ and F$_B^-$. Regardless of the mechanism, a PS I−molecular wire−Pt nanoparticle bioconjugate that incorporated all of these changes resulted in a light-induced rate of 312 μmol of H$_2$ (mg of Chl)$^{-1}$ h^{-1} (*68*).

This approach of directly coupling the photochemical module to a catalytic module via a molecular wire for the photocatalytic production of H$_2$ creates new possibilities in bioenergy research. We currently assume that the electron quantum mechanically tunnels between the [4Fe-4S] cluster and the Pt nanoparticle through σ and, where they exist, π bonds of the molecular wire. Electron transfer has been shown to occur on the picosecond time scale when fully conjugated wires with lengths between 6.6 and 28 Å are employed (*69*). The molecular wires employed in Table 1 are either fully saturated or less than fully conjugated; however, their lengths are significantly shorter than those studied by Sikes et al. (*69*). Alternatively, the molecular wires may simply tether the two redox centers together at sufficiently short distances that the electron quantum mechanically tunnels through space (the aqueous medium) between the [4Fe-4S]$^+$ cluster and the surface of the Pt nanoparticle. Given that the through-space distance may change with time due to the flexibility of the molecular wire, a combination of through-bond and through-space electron transfer is probably realistic. Future work will be required to decide which of these two mechanisms is dominant. With the direct linking of PS I, the photochemical module, to Au and Pt nanoparticles, the catalytic module, diffusion of an intermediate
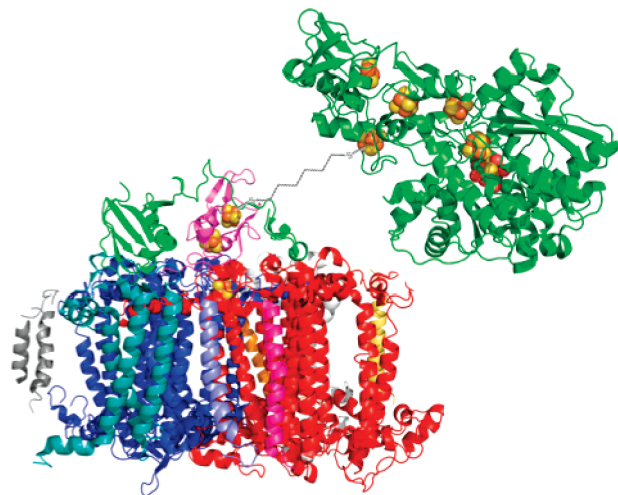
FIGURE 7: Depiction of the PS I−molecular wire−[FeFe]-H_2ase construct. The molecular wire is 1,6-hexanedithiol. For the sake of clarity, the molecular wire is not scaled to the same dimension as the proteins.

electron transfer carrier was eliminated while the native structure and electron transfer properties of PS I were well preserved.

PHOTOSYSTEM I−MOLECULAR WIRE−H_2ASE CONSTRUCTS

In a manner similar to that for the Pt nanoparticles, the HydA protein of [FeFe]-H_2ase from *C. acetobutylicum* was wired to the PsaC protein of PS I (C. E. Lubner, P. Silva, D. A. Bryant, and J. H. Golbeck, manuscript in preparation). The second Cys residue in the cluster binding motif (Cys_{97}) for the surface-located, distal [4Fe-4S] cluster of [FeFe]-H_2ase was changed by site-specific mutagenesis to Gly to create a similarly differentiated coordination site. When the *hydA* gene encoding this variant was coexpressed in *E. coli* with the *hydEFG* maturation genes from *C. acetobutylicum*, some partially active HydA(Cys_{97}Gly) variant enzyme was produced. When the variant HydA was compared with wild-type HydA through cyclic voltammetry, no noticeable changes were observed in the shape of the voltammograms, indicating that the mode of electron transfer to and from the active site had not been altered significantly (K. Vincent, personal communication). However, a noticeable decrease in the H_2 evolution activity of the variant enzyme was observed; the variant enzyme had an activity of 11.5 mol of H_2 (mol of H_2ase)$^{-1}$ s^{-1}, while the wild-type enzyme had an activity of 80.6 mol of H_2 (mol of H_2ase)$^{-1}$ s^{-1}.

The F_B cluster of the Cys_{13}Gly variant of PsaC on PS I was covalently linked to the distal [4Fe-4S] cluster of the Cys_{97}Gly variant of the HydA enzyme using 1,6-hexanedithiol as the molecular wire (Figure 7). Because of the oxygen sensitivity of [FeFe]-H_2ases, assembly of the PS I−molecular wire−H_2ase construct was performed under strictly anaerobic conditions. Soluble electron donors, Cyt c_6, ascorbate, and DPIP, were added to a dark-adapted sample, and light-induced H_2 production occurred at a rate of 3.9 μmol of H_2 (mg of Chl)$^{-1}$ h^{-1}. This rate is approximately 10-fold higher than those previously achieved by other groups using (only) biological components. Moreover, this PS I−molecular wire−H_2ase construct has proven to be remarkably stable: the activity of this construct has remained more or less constant when stored for greater than 2 months at room temperature under anoxic conditions.

Table 2: Comparative Rates of Light-Induced Production of Hydrogen from Inorganic and Proteinaceous Catalytic Systems

	rate of H_2 production [μmol of H_2 (mg of Chl)$^{-1}$ h^{-1}]
metal systems	
platinized PS I[a]	0.025
PC-cross-linked platinized PS I	0.080
osmium-coated chloroplasts	0.113
PS I−molecular wire−Au nanoparticle[a]	3.4
PS I−molecular wire−Pt nanoparticle[a]	9.6
PS I−molecular wire−Pt nanoparticle with Cyt c[a]	49.3
PS I−molecular wire−Pt nanoparticle (optimized)	312
proteinaceous systems	
PS I−H_2ase[a]	0.58
PS I−molecular wire−H_2ase[a]	3.9

[a]Soluble electron donors used.

The PS I−molecular wire−H_2ase construct can be further optimized. As described above, this can be achieved by cross-linking the native electron donor to PS I, by changing the length and conjugation of the wire, and by using a much more active H_2ase. The length and conjugation of the molecular wire are important for bringing the two modules sufficiently close together to transfer an electron efficiently on the relevant time scale. While the proposed pathway for electron transfer is through the molecular wire (see discussion above), the possibility exists for direct tunnelling between the F_B cluster of PsaC and the distal [4Fe-4S] cluster of H_2ase. If the latter mechanism is correct, shorter wires might result in increased H_2 production rates regardless of the mechanism of electron transfer, whereas aromatic wires may not have a significant effect.

CONCLUSIONS AND FURTHER CONSIDERATIONS

The direct coupling of H_2ases to PS I currently has promise for producing the highest rates of H_2 evolution by eliminating the diffusion-based step in electron transfer. The high absorption efficiency and quantum yield, favorable redox properties, and relatively long-term stability properties of PS I allow it to be coupled with a catalytic module to create a device that is capable of high rates of H_2 production when illuminated (Table 2). Improvement of the device requires the development of more active H_2ase enzymes, especially in variants, which were shown to have significantly reduced catalytic activity. While the noble metal-based systems discussed here generate H_2 at significant rates, these devices ultimately pose a challenge because of the high cost and low natural abundance of precious metals. Because the catalyst metals in biological H_2ase systems, i.e., iron and nickel, are relatively inexpensive and abundant, they may serve as the basis for the design of cheap and thus more competitive solar H_2 devices. The current design strategy involves docking the PS I−molecular wire−H_2ase construct on a gold electrode to generate a cathodic photochemical half-cell. However, provided that an appropriate dithiol compound can be produced in living cells, a similar methodology could eventually be used to connect PS I with H_2ase in vivo or to connect PS I to other redox proteins that have surface-located [4Fe-4S] clusters. Via combination of different approaches, a highly efficient photosynthetic H_2 device may become a realistic technology for replacing fossil fuels as a significant source of stored chemical energy.

The modular nature of these systems may also allow this device to be used as a test bed for both artificial photosynthetic systems and synthetic H₂ases. Although progress has been made in the design of catalysts capable of proton reduction, candidate catalysts that could effectively replace Au and Pt are not yet available. However, as synthetic catalysts for H_2 generation are developed, they could be used as the catalytic module in place of Pt or H₂ase. Similarly, as high-quantum yield artificial photosynthetic devices with the necessary attributes become available, they could be used as the photochemical module in place of PS I. Another application of this system results from the ability to use light to control the injection of electrons one at a time into the active sites of redox-active enzymes that perform multielectron (proton-coupled) reduction reactions.

REFERENCES

1. Golbeck, J. H. (1993) Shared Thematic Elements in Photochemical Reaction Centers. *Proc. Natl. Acad. Sci. U.S.A. 90*, 1642–1646.
2. Heathcote, P., Jones, M. R., and Fyfe, P. K. (2003) Type I photosynthetic reaction centres: Structure and function. *Philos. Trans. R. Soc. London, Ser. B 358*, 231–243.
3. Grotjohann, I., and Fromme, P. (2005) Structure of cyanobacterial photosystem I. *Photosynth. Res. 85*, 51–72.
4. Golbeck, J. H. (2003) The Binding of Cofactors to Photosystem I Analyzed by Spectroscopic and Mutagenic Methods. *Annu. Rev. Biophys. Biomol. Struct. 32*, 237–256.
5. Amunts, A., and Nelson, N. (2008) Functional organization of a plant Photosystem I: Evolution of a highly efficient photochemical machine. *Plant Physiol. Biochem. 46*, 228–237.
6. Jordan, P., Fromme, P., Witt, H. T., Klukas, O., Saenger, W., and Krauss, N. (2001) Three dimensional structure of Photosystem I at 2.5 Å resolution. *Nature 411*, 909–917.
7. Golbeck, J. H. (2004) Photosynthetic Reaction Centers. In Energy Transduction in Membranes (Cramer, W., Ed.) Biophysical Society, Bethesda, MD.
8. Moser, C. C., Page, C. C., Cogdell, R. J., Barber, J., Wraight, C. A., and Dutton, P. L. (2003) Length, time, and energy scales of photosystems. *Adv. Protein Chem. 63*, 71–109.
9. Lien, S., and San Pietro, A. (1971) An Inquiry into Biophotolysis of Water to Produce Hydrogen. In A report sponsored by NSF under Research Applied to National Needs (RANN) Grant IG 40253 to Indiana University.
10. Gibbs, M., Hollaender, A., Kok, B., Krampitz, L. O., and San Pietro, A. (1973) Proceedings of the Workshop on Bio-Solar Conversion. In A report on a workshop held 5–6 September 1973 at Bethesda, MD supported by NSF under RANN Grant GI 40253 to Indiana University.
11. Ke, B., Hansen, R. E., and Beinert, H. (1973) Oxidation-reduction potentials of bound iron-sulfur proteins of photosystem I. *Proc. Natl. Acad. Sci. U.S.A. 70*, 2941–2945.
12. Heathcote, P., Williams-Smith, D. L., Sihra, C. K., and Evans, M. C. W. (1978) The role of the membrane-bound iron-sulfur centers A and B in the photosystem I reaction centre of spinach chloroplasts. *Biochim. Biophys. Acta 503*, 333–342.
13. Terashima, I., Funayama, S., and Sonoike, K. (1994) The Site of Photoinhibition in Leaves of *Cucumis sativus* L. at Low Temperatures Is Photosystem I, Not Photosystem II. *Planta 193*, 300–306.
14. Sonoike, K., Terashima, I., Iwaki, M., and Itoh, S. (1995) Destruction of Photosystem I Iron-Sulfur Centers in Leaves of *Cucumis sativus* L. by Weak Illumination at Chilling Temperatures. *FEBS Lett. 362*, 235–238.
15. Terashima, I., Noguchi, K., ItohNemoto, T., Park, Y. M., Kubo, A., and Tanaka, K. (1998) The cause of PSI photoinhibition at low temperatures in leaves of *Cucumis sativus*, a chilling-sensitive plant. *Physiol. Plant. 103*, 295–303.
16. Parrett, K. G., Mehari, T., Warren, P. G., and Golbeck, J. H. (1989) Purification and properties of the intact P-700 and Fx-containing photosystem I core protein. *Biochim. Biophys. Acta 973*, 324–332.
17. Golbeck, J. H., Parrett, K. G., Mehari, T., Jones, K. L., and Brand, J. J. (1988) Isolation of the intact photosystem I reaction center core containing P700 and iron-sulfur center FX. *FEBS Lett. 228*, 268–272.
18. Li, N., Warren, P. V., Golbeck, J. H., Frank, G., Zuber, H., and Bryant, D. A. (1991) Polypeptide composition of the Photosystem I complex and the Photosystem I core protein from *Synechococcus* sp. PCC 6301. *Biochim. Biophys. Acta 1059*, 215–225.

19. Golbeck, J. H., Mehari, T., Parrett, K., and Ikegami, I. (1988) Reconstitution of the photosystem I complex from the P700 and FX-containing reaction center core protein and the FA/FB polypeptide. *FEBS Lett. 240*, 9–14.
20. Parrett, K. G., Mehari, T., and Golbeck, J. H. (1990) Resolution and Reconstitution of the Cyanobacterial Photosystem I Complex. *Biochim. Biophys. Acta 1015*, 341–352.
21. Zhao, J., Warren, P. V., Li, N., Bryant, D. A., and Golbeck, J. H. (1990) Reconstitution of electron transport in photosystem I with PsaC and PsaD proteins expressed in *Escherichia coli*. *FEBS Lett. 276*, 175–180.
22. Li, N., Zhao, J., Warren, P., Warden, J., Bryant, D., and Golbeck, J. (1991) PsaD Is Required for the Stable Binding of PsaC to the Photosystem I Core Protein of *Synechococcus* sp. PCC 6301. *Biochemistry 30*, 7863–7872.
23. Zhao, J. D., Li, N., Warren, P. V., Golbeck, J. H., and Bryant, D. A. (1992) Site-directed conversion of a cysteine to aspartate leads to the assembly of a [3Fe-4S] cluster in PsaC of Photosystem I: The photoreduction of F_A is independent of F_B. *Biochemistry 31*, 5093–5099.
24. Golbeck, J. H., and Cornelius, J. M. (1986) Photosystem I charge separation in the absence of centers A and B. I. Optical characterization of center 'A₂' and evidence for its association with a 64-kDa polypeptide. *Biochim. Biophys. Acta 849*, 16–24.
25. Warden, J. T., and Golbeck, J. H. (1986) Photosystem I charge separation in the absence of centers A and B. II. ESR spectral characterization of center 'X' and correlation with optical signal 'A2'. *Biochim. Biophys. Acta 849*, 25–31.
26. Golbeck, J. H., Parrett, K. G., and McDermott, A. E. (1987) Photosystem I charge separation in the absence of center A and B. III. Biochemical characterization of a reaction center particle containing P-700 and FX. *Biochim. Biophys. Acta 893*, 149–160.
27. Golbeck, J. H., Parrett, K. G., and Root, L. L. (1987) Photosystem I charge separation in the absence of centers A and B: Biochemical characterization of the stabilized P700 A2(X) reaction center. In Progress in Photosynthesis Research, Proceedings of the 7th International Congress on Photosynthesis (Biggins, J., Ed.) Vol. 1, pp 253−256, Nijhoff: Dordrecht, The Netherlands.
28. Van der Est, A., Valieva, A. I., Kandrashkin, Y. E., Shen, G., Bryant, D. A., and Golbeck, J. H. (2004) Removal of PsaF alters forward electron transfer in Photosystem I: Evidence for fast reoxidation of Q_KA in subunit deletion mutants of *Synechococcus* sp. PCC 7002. *Biochemistry 43*, 1264–1275.
29. Yang, F., Shen, G., Schluchter, W. M., Zybailov, B., Ganago, A. O., Vassiliev, I. R., Bryant, D. A., and Golbeck, J. H. (1998) Deletion of the PsaF polypeptide modifies the environment of the redox-active phylloquinone. Evidence for unidirectionality of electron transfer in Photosytem I. *J. Phys. Chem. B 102*, 8288–8299.
30. Golbeck, J. H. (1999) A comparative analysis of the spin state distribution of in vivo and in vitro mutants of PsaC. A biochemical argument for the sequence of electron transfer in Photosystem I as $FX \rightarrow FA \rightarrow FB \rightarrow$ ferredoxin/flavodoxin. *Photosynth. Res. 61*, 107–149.
31. Zirngibl, C., Vandongen, W., Schworer, B., Vonbunau, R., Richter, M., Klein, A., and Thauer, R. K. (1992) H₂ Forming Methylenetetrahydromethanopterin Dehydrogenase, a Novel Type of Hydrogenase without Iron-Sulfur Clusters in Methanogenic Archaea. *Eur. J. Biochem. 208*, 511–520.
32. Lyon, E. J., Shima, S., Boecher, R., Thauer, R. K., Grevels, F. W., Bill, E., Roseboom, W., and Albracht, S. P. (2004) Carbon monoxide as an intrinsic ligand to iron in the active site of the iron-sulfur-cluster-free hydrogenase H₂ forming methylenetetrahydromethanopterin dehydrogenase as revealed by infrared spectroscopy. *J. Am. Chem. Soc. 126*, 14239–14248.
33. Lyon, E. J., Shima, S., Buurman, G., Chowdhuri, S., Batschauer, A., Steinbach, K., and Thauer, R. K. (2004) UV-A/blue-light inactivation of the 'metal-free' hydrogenase (Hmd) from methanogenic archaea. *Eur. J. Biochem. 271*, 195–204.
34. Shima, S., Lyon, E. J., Sordel-Klippert, M., Kauss, M., Kahnt, J., Thauer, R. K., Steinbach, K., Xie, X., Verdier, L., and Griesinger, C. (2004) The cofactor of the iron-sulfur cluster free hydrogenase hmd: Structure of the light-inactivation product. *Angew. Chem., Int. Ed. 43*, 2547–2551.
35. Shima, S., and Thauer, R. K. (2007) A third type of hydrogenase catalyzing H₂ activation. *Chem. Rec. 7*, 37–46.
36. Fontecilla-Camps, J. C. (2009) Structure-function relationships of hydrogenases. *Amino Acids 37*, 22–23.
37. McGlynn, S. E., Shepard, E., Ruebush, S., Broderick, J. B., and Peters, J. W. (2009) [FeFe] Hydrogenases: A Modern Bio-catalytic Link to Ancient Geochemistry. *Origins Life Evol. Biosphere 39*, 319–320.

38. McGlynn, S. E., Mulder, D. W., Shepard, E. M., Broderick, J. B., and Peters, J. W. (2009) Hydrogenase cluster biosynthesis: Organometallic chemistry nature's way. *Dalton Trans. 45*, 4274–4285.
39. Blokesch, M., and Bock, A. (2006) Properties of the [NiFe]-hydrogenase maturation protein HypD. *FEBS Lett. 580*, 4065–4068.
40. Vignais, P. M., and Colbeau, A. (2004) Molecular biology of microbial hydrogenases. *Curr. Issues Mol. Biol. 6*, 159–188.
41. Happe, T., and Naber, J. D. (1993) Isolation, Characterization and N-Terminal Amino Acid Sequence of Hydrogenase from the Green Alga *Chlamydomonas reinhardtii*. *Eur. J. Biochem. 214*, 475–481.
42. Happe, T., Mosler, B., and Naber, J. D. (1994) Induction, localization and metal content of hydrogenase in the green alga *Chlamydomonas reinhardtii*. *Eur. J. Biochem. 222*, 769–774.
43. Pilet, E., Nicolet, Y., Mathevon, C., Douki, T., Fontecilla-Camps, J. C., and Fontecave, M. (2009) The role of the maturase HydG in [FeFe]-hydrogenase active site synthesis and assembly. *FEBS Lett. 583*, 506–511.
44. King, P. W., Posewitz, M. C., Ghirardi, M. L., and Seibert, M. (2006) Functional Studies of [FeFe] Hydrogenase Maturation in an *Escherichia coli* Biosynthetic System. *J. Bacteriol. 188*, 2163–2172.
45. Winter, G., Buhrke, T., Lenz, O., Jones, A. K., Forgber, M., and Friedrich, B. (2005) A model system for [NiFe] hydrogenase maturation studies: Purification of an active site-containing hydrogenase large subunit without small subunit. *FEBS Lett. 579*, 4292–4296.
46. Greenbaum, E. (1985) Platinized Chloroplasts: A Novel Photocatalytic Material. *Science 230*, 1373–1375.
47. Greenbaum, E. (1988) Interfacial photoreactions at the photosynthetic membrane interface: An upper limit for the number of platinum atoms required to form a hydrogen-evolving platinum metal complex. *J. Phys. Chem. 92*, 4571–4574.
48. Lee, J. W., Tevault, C. V., Blankinship, S. L., Collins, R. T., and Greenbaum, E. (1994) Photosynthetic water-splitting: In-situ photoprecipitation of metallocatalysts for photoevolution of hydrogen and oxygen. *Energy Fuels 8*, 770–773.
49. Lee, J. W., Lee, I., and Greenbaum, E. (2005) Imaging Nanometere Metallocatalysts Formed by Photosynthetic Deposition of Water-Soluble Transition-Metal Compounds. *J. Phys. Chem. B 109*, 5409–5413.
50. Millsaps, J. F., Bruce, B. D., Lee, J. W., and Greenbaum, E. (2001) Nanoscale photosynthesis: Photocatalytic production of hydrogen by platinized photosystem I reaction centers. *Photochem. Photobiol. 73*, 630–635.
51. Evans, B. R., O'Neill, H. M., Hutchens, S. A., Bruce, B. D., and Greenbaum, E. (2004) Enhanced photocatalytic hydrogen evolution by covalent attachment of plastocyanin to photosystem I. *Nano Lett. 4*, 1815–1819.
52. Ihara, M., Nishihara, H., Yoon, K. S., Lenz, O., Friedrich, B., Nakamoto, H., Kojima, K., Honma, D., Kamachi, T., and Okura, I. (2006) Light-driven hydrogen production by a hybrid complex of a [NiFe]-hydrogenase and the cyanobacterial photosystem I. *Photochem. Photobiol. 82*, 676–682.
53. Schubert, T., Lenz, O., Krause, E., Volkmer, R., and Friedrich, B. (2007) Chaperones specific for the membrane-bound [NiFe]-hydrogenase interact with the Tat signal peptide of the small subunit precursor in *Ralstonia eutropha* H16. *Mol. Microbiol. 66*, 453–467.
54. Itoh, S., Iwaki, M., and Ikegami, I. (2001) Modification of Photosystem I reaction center by the extraction and exchange of chlorophylls and quinones. *Biochim. Biophys. Acta 1507*, 115–138.
55. Terasaki, N., Yamamoto, N., Hiraga, T., Yamanoi, Y., Yonezawa, T., Nishihara, H., Ohmori, T., Sakai, M., Fujii, M., Tohri, A., Iwai, M., Inoue, Y., Yoneyama, S., Minakata, M., and Enami, I. (2009) Plugging a Molecular Wire into Photosystem I: Reconstitution of the Photoelectric Conversion System on a Gold Electrode. *Angew. Chem., Int. Ed. 48*, 1585–1587.
56. Terasaki, N., Yamamoto, N., Tamada, K., Hattori, M., Hiraga, T., Tohri, A., Sato, I., Iwai, M., Taguchi, S., Enami, I., Inoue, Y., Yamanoi, Y., Yonezawa, T., Mizuno, K., Murata, M., Nishihara, H., Yoneyama, S., Minakata, M., Ohmori, T., Sakai, M., and Fujii, M. (2007) Bio-photosensor: Cyanobacterial photosystem I coupled with transistor via molecular wire. *Biochim. Biophys. Acta 1767*, 653–659.
57. Jung, Y. S., Vassiliev, I. R., Yu, J. P., McIntosh, L., and Golbeck, J. H. (1997) Strains of *Synechocystis* sp. PCC 6803 with altered PsaC 0.2. EPR and optical spectroscopic properties of F-A and F-B in aspartate, serine, and alanine replacements of cysteines 14 and 51. *J. Biol. Chem. 272*, 8040–8049.
58. Yu, J. P., Vassiliev, I. R., Jung, Y. S., Golbeck, J. H., and McIntosh, L. (1997) Strains of *Synechocystis* sp. PCC 6803 with altered PsaC 0.1. Mutations incorporated in the cysteine ligands of the two [4Fe-4S] clusters F-A and F-B of photosystem I. *J. Biol. Chem. 272*, 8032–8039.
59. Jung, Y. S., Vassiliev, I. R., Qiao, F. Y., Yang, F., Bryant, D. A., and Golbeck, J. H. (1996) Modified ligands to F_A and F_B in Photosystem I: Proposed chemical rescue of a [4Fe-4S] cluster with an external thiolate in alanine, glycine, and serine mutants of PsaC. *J. Biol. Chem. 271*, 31135–31144.
60. Yu, L., Zhao, J. D., Lu, W. P., Bryant, D. A., and Golbeck, J. H. (1993) Characterization of the [3Fe-4S] and [4Fe-4S] Clusters in Unbound PsaC Mutants C14D and C51D: Midpoint Potentials of the Single [4Fe-4S] Clusters Are Identical to F(A) and F(B) in Bound PsaC of Photosystem I. *Biochemistry 32*, 8251–8258.
61. Mehari, T., Qiao, F. Y., Scott, M. P., Nellis, D. F., Zhao, J. D., Bryant, D. A., and Golbeck, J. H. (1995) Modified ligands to F-A and F-B in photosystem I. 1. Structural constraints for the formation of iron-sulfur clusters in free and rebound PsaC. *J. Biol. Chem. 270*, 28108–28117.
62. Yu, L., Bryant, D. A., and Golbeck, J. H. (1995) Evidence for a mixed-ligand [4Fe-4S] cluster in the C14D mutant of PsaC. Altered reduction potentials and EPR spectral properties of the F_A and F_B clusters on rebinding to the P700-F_X core. *Biochemistry 34*, 7861–7868.
63. Yu, L., Vassiliev, I. R., Jung, Y. S., Bryant, D. A., and Golbeck, J. H. (1995) Modified ligands to F_A and F_B in Photosystem I. II. Characterization of a mixed ligand [4Fe-4S] cluster in the C51D mutant of PsaC upon rebinding to P700-F_X cores. *J. Biol. Chem. 270*, 28118–28125.
64. Antonkine, M. L., Maes, E. M., Czernuszewicz, R. S., Breitenstein, C., Bill, E., Falzone, C. J., Balasubramanian, R., Lubner, C., Bryant, D. A., and Golbeck, J. H. (2007) Chemical rescue of a site-modified ligand to a [4Fe-4S] cluster in PsaC, a bacterial-like dicluster ferredoxin bound to Photosystem I. *Biochim. Biophys. Acta 1267*, 712–724.
65. Jin, Z., Heinnickel, M., Krebs, C., Shen, G., Golbeck, J. H., and Bryant, D. A. (2008) Biogenesis of iron-sulfur clusters in photosystem I: Holo-NfuA from the cyanobacterium *Synechococcus* sp. PCC 7002 rapidly and efficiently transfers [4Fe-4S] clusters to apo-PsaC in vitro. *J. Biol. Chem. 283*, 28426–28435.
66. Que, L., Jr., Bobrick, M. A., Ibers, J. A., and Holm, R. (1974) Synthetic Analogs of Active Sties of Iron-Sulfur Proteins. VII. Ligand Substitution Reactions of the Tetranuclear Clusters $[Fe_4S_4(SR)_4]^{2-}$ and the structure of $[(CH_3)_4N]_2 [Fe_4S_4(SC_6H_6)_4]$. *J. Am. Chem. Soc. 96*, 4168–4177.
67. Grimme, R. A., Lubner, C. E., Bryant, D. A., and Golbeck, J. H. (2008) Photosystem I/molecular wire/metal nanoparticle bioconjugates for the photocatalytic production of H_2. *J. Am. Chem. Soc. 130*, 6308–6309.
68. Grimme, R. A., Lubner, C. E., and Golbeck, J. H. (2009) Maximizing H_2 production in Photosystem I/dithiol molecular wire/platinum nanoparticle bioconjugates. *Dalton Trans. 45*, 10106–10113.
69. Sikes, H. D., Smalley, J. F., Dudek, S. P., Cook, A. R., Newton, M. D., Chidsey, C. E. D., and Feldberg, S. W. (2001) Rapid Electron Tunneling Through Oligophenylenevinylene Bridges. *Science 291*, 1519–1523.